Water Research 214 (2022) 118210

Contents lists available at ScienceDirect

Water Research

journal homepage: www.elsevier.com/locate/watres

A novel strategy for rapid development of a self-sustaining symbiotic algal-bacterial granular sludge: Applying algal-mycelial pellets as nuclei

Bing Zhang [a,*], Lian Wu [a], Wenxin Shi [a], Zhiqiang Zhang [b], Piet N.L. Lens [c]

[a] College of Environment and Ecology, Chongqing University, Chongqing 400044, China
[b] School of Environmental and Municipal Engineering, Xi'an University of Architecture and Technology, Xi'an 710055, China
[c] UNESCO-IHE, Institute for Water Education, Westvest 7, DA Delft 2601, the Netherlands

ARTICLE INFO

Keywords:
Algal-bacterial granular sludge (ABGS)
Mycelial pellets
Extracellular polymeric substances (EPS)
Mechanism analysis
XDLVO theory
Community structure

ABSTRACT

Algal-bacterial granular sludge (ABGS) is a promising technology for wastewater treatment, benefiting from the synergetic interactions between algae and bacteria. However, the rapid start-up of the ABGS system is not trivial. Herein, a novel strategy was proposed by applying the algal-mycelial pellets (AMPs) as the primary nuclei for accelerating the development of a self-sustaining symbiotic ABGS system. The results indicated that by using this strategy complete granulation was shortened to 12 days, much shorter than the control system without AMPs dosage (28 days). The ABGS had a large particle diameter (3.3 mm), compact granular structure (1.0253 g/mL), and excellent settleability (SVI_{30} of 53.2 mL/g). Moreover, 98.6% of COD, 80.8% of TN and 80.0% of PO_4^{3-}-P were removed by the ABGS. The nuclei of targeted algae (*Chlorella*) and filamentous fungi (*Aspergillus niger*), the enhanced production of extracellular polymeric substances (especially proteins) and the enrichment of functional bacteria (such as *Neomegalonema* and *Flavobacterium*) facilitated the granules development. The low surface free energy (-69.56 mJ/m^2) and energy barrier (89.93 KT) were the inherent mechanisms for the strong surface hydrophobicity, the easy bacterial adhesion, and the short granulation period. This study provides an economically feasible approach to accelerate ABGS granulation and sustain system stability.

1. Introduction

Algal-bacterial granular sludge (ABGS) as an environmental sustainable and economically viable platform for municipal wastewater treatment has aroused extensive research in recent years (Ji and Liu, 2022). Previous studies indicated that the ABGS are a promising alternative for the conventional bacteria-based aerobic granular sludge (AGS), with a denser structure, higher biomass yield, better settling capacity, and superior nutrient removal (Ahmad et al., 2017). In such a symbiotic system, algae provide oxygen via photosynthesis to bacteria for organic matter oxidization, whereas the bacteria produce carbon dioxide to algae for photosynthesis. Benefiting from the synergetic interactions between algae and bacteria, the energy consumption related to external aeration can be substantially reduced in the ABGS system. Specifically, the recoverable energy from anaerobic digestion of ABGS biomass was enough to offset the energy consumption (associated with aeration and sludge separation), and a net energy gain of 64.1 billion kWh/yr was estimated for an ABGS system treating municipal wastewater, with less greenhouse gases (GHGs) emissions (60.2 million tons CO_2e/yr) (Zhang et al., 2021).

Achieving rapid granulation of ABGS to take advantage of algae-bacteria symbiotic relationships is essential for sustaining the excellent process performance (Ji et al., 2020). Past attempts to cultivate ABGS mainly focused on exposure of activated sludge to a natural or artificial day-light regime to induce spontaneous growth of algae (He et al., 2018a), or inoculation with targeted algae (such as *Chlorella* or *Scenedesmus*) (Liu et al., 2018). However, a long reaction time (up to 2 months) was required to achieve complete granulation of ABGS (Zhang et al., 2018). The high energy consumption and low nutrient removal efficiency during the granulation process compromised the merits of this promising technology. Up to now, most research regarding the ABGS system centered on the effects of influencing factors, e.g. light intensity, salinity and temperature (Meng et al., 2019a; Meng et al., 2019b), reactor configuration (Ahmad et al., 2017), granular stability (Zhao et al., 2019b), pollutants or nutrient removal efficiencies and mechanisms involved (Zhao et al., 2018). Only few studies emphasized the most crucial and difficult issue, i.e. shortening the start-up period for the granulation of ABGS. As an example, it was stated that rapid

* Corresponding author.
E-mail address: zhangbing@cqu.edu.cn (B. Zhang).

https://doi.org/10.1016/j.watres.2022.118210
Received 25 October 2021; Received in revised form 18 January 2022; Accepted 16 February 2022
Available online 19 February 2022

establishment of ABGS system could be realized within 18 days, but pre-culturing mature ABGS to serve as the inoculum sludge was still required (Zhang et al., 2020b).

The formation mechanism of ABGS might provide a new insight for the rapid granulation. When algae cells coalesce with each other, small agglomerates are formed that act as nuclei for microbial adhesion during the primary stage of ABGS formation (detailed morphology see Fig. S1), which was a very crucial step to initiation of granule development (Zhang et al., 2018; Zhang et al., 2022). Similarly, Ahmad et al., (2017) confirmed this, stating that in a growth environment with high water velocity, algae cells tended to accumulate in the interior of ABGS as the core, and this unique structure was beneficial for sustaining granular stability. These studies indicate that, different from the anaerobic core in AGS, ABGS are comprised of algae nuclei, which challenges the general assumption that algae tend to grow on the AGS surface on account of photosynthesis, but this phenomenon is often overlooked. Inspired by these findings, it is thus inferred that rapid formation of primary algae nuclei will accelerate the development of ABGS. Nonetheless, to the best of our knowledge, this remains up to now an unexplored field.

Generally, the undesirable properties of algae cells, including small cell size, poor settling ability, slow growth rate and strong electrostatic repulsion, make it challenging to form the primary nuclei of ABGS via algal self-aggregation. This issue can be tackled by a pelletization strategy based on co-culture of algae and fungi. Filamentous fungi have different morphology in liquid media, including spores, mycelium and clumps (Metz and Kossen, 1977). Thereinto, the spores can germinate to form intertwined mycelia and even spherical mycelial aggregates with loose interior and dense surface, which are called mycelial pellets (MPs) (Li et al., 2020). When co-cultivating algae with fungi, algal cells can be rapidly immobilized in the fungal pellets by entrapment in the MPs or by attachment to the fungal filaments (usually 1-3 d), thus forming the algal-mycelial pellets (AMPs) (Li et al., 2017). This process is easy to operate, with high bio-flocculation efficiency (90%-99%) and low operational costs (Zhao et al., 2019a). Notably, the fungi-associated pelletization has been extensively studied in promoting bio-flocculation of algae cells for wastewater treatment and biofuel production. Yet, whether the pelletized algae-mycelial biomass (i.e. AMPs) can provide the primary nuclei for the ABGS has not been investigated.

In this context, this work aimed to investigate the feasibility of utilizing AMPs as the primary nuclei for rapid start-up of a self-sustaining ABGS system with respect to (i) key parameter optimization for AMPs biosynthesis, (ii) the granulation process and synergistic algal-bacterial bioconversions in the ABGS system, (iii) characteristics of the micromorphology, extracellular polymeric substance (EPS), and community structure dynamics (bacteria, algae and fungi) of the ABGS, (iv) the surface interaction energy of granular sludge cells and sludge aggregation capacity based on the extended Derjaguin-Landau-Verwey-Overbeek (XDLVO) theory, and (v) practical implication of this study. The results provide a novel and economically feasible strategy to tackle the long start-up of ABGS systems, while shedding light on further engineering applications of ABGS for cost-effective and environmentally sustainable municipal wastewater treatment.

2. Methods and materials

2.1. Preparation of MPs and AMPs

Aspergillus niger (AS3.3928), a filamentous pellet-forming fungal strain with high flocculation activity, was purchased from the China General Microbiological Culture Collection Center (Beijing, China). It was incubated in potato dextrose agar (PDA) and sub-cultured at 37°C until spores were produced (Li et al., 2017). The spores were scraped from the PDA plate and placed into a glass flask (250 mL) with sterile water (100 mL) to prepare the spore suspensions. The concentration of spore suspensions was adjusted to 10^6 spores/mL and inoculated in a sterile liquid Czapek medium to obtain MPs (Yu et al., 2020).

A non-flocculating algae strain of *Chlorella* (FACHB-31) was obtained from the Freshwater Algae Culture Collection at the Institute of Hydrobiology (Wuhan, China). *Chlorella* was cultivated in BG11 medium under a 12 h light/12 h dark cycle at 25°C, then taken out at the logarithmic phase. The density of algal cells was adjusted to 8.5×10^6 cell/L for further studies.

Two methods were utilized to prepare AMPs: the co-cultivation method (based on the spore-assisted mode) and the adsorption method (based on the pellet-assisted mode) (Chen et al., 2018). As for the former method, fresh spores of the candidate fungal strains were inoculated into the suspension of *Chlorella* and then germinated to form the AMPs; while the later method dosed the pre-cultured MPs into the suspension of *Chlorella*. After the flocculation of *Chlorella*, the flocculation efficiency was evaluated by a spectrometer (DR6000, HACH, USA) at a wavelength of 680 nm. The flocculation efficiency was calculated according to Eq. (1):

Flocculation efficiency (%) $= (C_0-C_t)/C_0\times100$ (1) where $C_0 = OD_{680}$ at the initial stage, $C_t = OD_{680}$ after t hour.

2.2. Experimental set-up and operation

Three photo-reactors with an effective working volume of 400 mL were used for the development of ABGS (Fig. S2). They were shaken constantly at 150 rpm and 25°C. R1 was operated as a control by inoculating with *Chlorella* and activated sludge. R2 was inoculated with MPs, *Chlorella* and activated sludge, whereas R3 was inoculated with AMPs and activated sludge. Illumination of the three photo-reactors was provided by LED lamps (Philips, 40 W, Germany). The average photometric intensity inside the three reactors was controlled at 4500 (± 200) lux with a constant 12 h dark/12 h light cycle. The operational cycling time was 12 h, which included 1 min filling, 712-716 min shaking, 1-5 min settling, and 2 min discharging. Before discharging, the shaker was stopped for sludge settling, and subsequently, two hundred milliliters of the upper mixed solution were discharged using a peristaltic pump (BT600M, Chuang Rui, China). The volume exchange rate was kept at 50%, resulting in a hydraulic retention time (HRT) of 24 h. The sludge retention time (SRT) was controlled at approximately 28 days according to the calculation formula provided in the Supplementary Materials (Text S1).

2.3. Inoculum sludge and synthetic wastewater

Jingkou Urban Wastewater Treatment Plant located at Chongqing (China) was selected as the sampling place for the activated sludge. The inoculum sludge was brown in color with a fluffy appearance and an average particle size of 82.1 μm. The sludge volume index at 30 min (SVI_{30}) was 54.0 mL/g.

The synthetic domestic wastewater was prepared according to Zhang et al., (2019). It contained 600 mg/L of COD (CH_3COONa), 60 mg/L of NH_4^+-N (NH_4Cl), 10 mg/L of PO_4^{3-}-P (KH_2PO_4/K_2HPO_4), 25 mg/L $MgSO_4{\cdot}7H_2O$, 30 mg/L $FeSO_4{\cdot}7H_2O$, 30 mg/L $CaCl_2$ and 1.0 mL/L trace element solution.

2.4. Analysis of EPS content and components

A thermal method for extracting the extracellular polymeric substances (EPS) was employed in conformity with a previous study (Zhang et al., 2019). Two main fractions of EPS, i.e. proteins (PN) and polysaccharides (PS), were quantified by the modified Lowery method (Peterson, 1977) and phenol-sulfuric acid method (Dubois et al., 1956), respectively. 3D-excitation-emission matrix (3D-EEM) spectra of the extracted EPS samples were analyzed by using a fluorescence spectrophotometer (F-4700, Hitachi, Japan). A parallel factor (PARAFAC) analysis was employed to handle the EEM data and identify the EPS components (Sheng et al., 2013).

2.5. Surface thermodynamics and XDLVO curve analysis

The zeta potential of ABGS was measured by using a zeta potential analyzer (Zetasizer Nano ZS90, Malvern, UK). For analysis of the contact angle, the sludge samples were broken using an ultrasonic cell disruptor (Xinyi-250N, China) at 20 kHz for 5 min, and the sludge suspension was diluted to 50 mL with deionized water. Subsequently, the suspensions were vacuum filtered onto 0.45 μm acetate cellulose membrane filters, followed by air drying at 25 ℃. A contact angle goniometer (Dataphysics OCA20, Germany) was used to measure the contact angles of sludge against distilled water, formamide, and diiodomethane. By measuring the contact angle of ABGS, the surface tension and interface free energy, the surface thermodynamic and the XDLVO curve of the ABGS can be analyzed. The detailed methods for surface thermodynamics analysis and XDLVO calculation are provided in the Supplementary Materials (Text S2).

2.6. High-throughput sequencing

The community compositions (bacteria, algae and fungi) of the inoculum sludge as well as the ABGS samples taken from R1-R3 on day 30 were evaluated using the high-throughput sequencing technology. The universal primer pairs 341F (5'-CCTACGGGNGGCWGCAG-3') and 805R (5'-GACTACHVGGGTATCTAATCC-3') were used to amplify the bacterial 16S rRNA region targeting the V3-V4 regions (Lu et al., 2015). The primer pairs P23SrV-1F (5'-GGACAGAAAGACCCTATGAA-3') and P23SrV-1R (5'-TCAGCCTGTTATCCCTAGAG-3') for algae were used for amplification of the hypervariable region of 18S rRNA (Zhang et al., 2020b). The specific primer sets with barcode ITS1F (5'-CTTGGT CATTTAGAGGAAGTAA-3') and ITS2R (5'-GCTGCGTTCTTCATC-GATGC-3') were employed to amplify the fungal ITS region (Gardes and Bruns, 1993). The detailed analytical methods were provided in a previous study (Guo et al., 2019).

2.7. Analytical methods

Mixed liquor (volatile) suspended solids (ML(V)SS), SVI_{30}, and the concentrations of COD, NH_4^+-N, NO_2^--N, NO_3^--N, TN and PO_4^{3-}-P in the influent and effluent were determined by standard methods (APHA, 2005). The chlorophyll α content was analyzed using the acetone extraction method (Ritchie, 2008).

Particle size was measured by a laser particle size analyzer (Malvern Panalytical Inc., Malvern, UK) and image J software. Morphology of the granules was observed using a scanning electron microscope (SEM, Quattro S, Thermo Scientific). The distribution of algae in the ABGS was observed by fluorescence microscopy through spontaneous fluorescence of chloroplast at 488 nm excitation wavelength. The distribution of nucleic acids, proteins, α-polysaccharides, and β-polysaccharides in the ABGS was visualized by using a confocal laser scanning microscope (CLSM, ZEISS Axio Scan. Z1, Germany).

The activities of functional bacteria, including ammonia oxidizing bacteria (SAUR), nitrite oxidation bacteria (SNUR) and heterotrophs (SOUR), were determined according to Huang et al., (2015). The ATPase activity was evaluated by a total ATPase kit (Nanjing, Jiancheng, China) as described by Jiang and Liu (2012).

2.8. Statistical analysis

All experiments were performed in triplicate. Significant differences in variables were ascertained using SPSS software (version 25.0, IBM), and a p value < 0.05 was regarded as a significant difference.

3. Results and discussion

3.1. Optimal biosynthesis conditions of MPs and AMPs

3.1.1. Preparation of MPs and AMPs at optimal conditions

The biosynthesis conditions of MPs were first optimized in this study. As shown in Fig. 1a, the growth of MPs sharply increased during the initial 72 h followed by a relatively saturated state. Besides, various factors that greatly influence the formation of MPs, including temperature, pH, rotary speed and initial inoculum spores density, were explored in this study. Results showed that thee biomass of MPs reached the maximal value when the cultivation conditions were controlled at an inoculum spores density of 6.3×10^6 CFU/mL, pH 6.0, rotary speed of 150 rpm, and 35°C (Fig. 1b e). Since it takes more energy to keep the temperature high and the operational temperature for ABGS is generally controlled at 25 30 °C, 30 °C was chosen as the optimal temperature for preparing the MPs.

The adsorption method and co-culture method to prepare the AMPs were comparatively investigated. It took respectively 12 h (adsorption method) and 24 h (co-culture method) to achieve complete flocculation of the algae (Fig. 1f,g). Besides, the AMPs prepared by the adsorption method were more numerous (Fig. 1l and Fig. S3), the adsorption method was, therefore, chosen for preparing the AMPs. The preparation conditions of AMPs were further optimized by evaluating the effects of the MPs cultivation period as well as the dosage amounts of MPs and algal cells on the flocculation efficiency Fig. 1.h j shows that the flocculation efficiency reached the maximal value of approximately 99.0% when dosing 50 mL algal cells (cell density of 8.5×10^6 cell/mL) and 12 g (wet weight) MPs which were pre-cultured for 72 h. The high flocculation efficiency was possibly due to the mediation of surface protein secreted by the MPs, the calcium bridging and the increase of hydrophobic interactions (Li et al., 2017).

The MPs obtained at the optimal conditions had a relatively loose boundary and compact kernel, with uniform size of approximately 1-2 mm (Fig. 1k). There was no conspicuous difference in morphology between MPs and AMPs, except for the color, which changed from white to green (Fig. 1l). *Chlorella* were closely attached onto the mycelium and mainly distributed in the outer layer of the AMPs, as revealed by SEM and TEM images (Fig. 1l). Furthermore, the long and dense mycelia intertwined with each other within AMPs, and correspondingly, channels and voids were formed on the surface, which may play a role of skeleton necessary for bacterial adhesion and the porous structure could facilitate mass transfer (Lahlali and Hijri, 2010). Therefore, it was speculated that the AMPs might be the ideal nuclei to enhance the development of ABGS.

3.1.2. Optimal mass ratio of AMPs and activated sludge

The mass ratio of AMPs and activated sludge, which plays a central role in affecting the aggregation ability of the ABGS, was investigated herein at the initial sludge concentration of 3.0 g/L MLSS. As shown in Fig. S4, the sludge amount adsorbed by AMPs decreased with further increase of the AMPs proportion. Besides, the AMPs gradually broke down or even vanished when the dry mass ratio of AMPs and activated sludge exceeded 2.5%. This may be attributed to the maladaptation of MPs to the environment in the bioreactor system, phagocytosis by metazoans or exfoliation caused by hydraulic shear, leading to AMPs disintegration (Fomina and Gadd, 2002). Therefore, the optimal mass ratio was determined at 2.5% (the ratio of dry weight of AMPs to that of activated sludge, w/w).

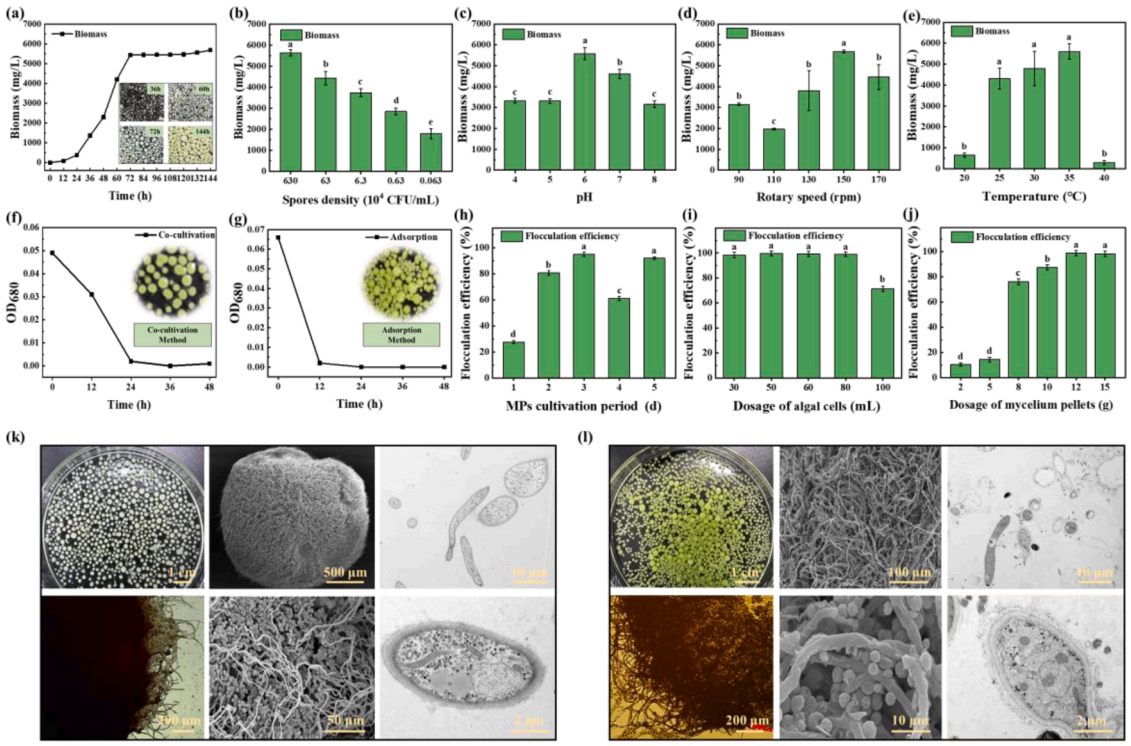

Fig. 1. Growth curve of MPs (inserted figure: representative images of MPs during the formation process) (a), the effects of inoculation spores density (b), pH (c), rotary speed (d), and temperature (e) on the formation of MPs. Variations of absorbance with time by using co-cultivation method (f) and adsorption method (g). The effects of the MPs cultivation period (h), dosage of algal cells (i), and dosage of MPs (j) on the formation of AMPs. Digital photographs, SEM and TEM images of MPs (k) and AMPs (l). Different letters signify significant differences ($p < 0.05$) and the same letters signify insignificant differences ($p > 0.05$).

3.2. Granulation process and ABGS morphology

3.2.1. Characteristics of ABGS

For development of the self-sustaining ABGS, the activated sludge (AS) was inoculated into the three photo-reactors to obtain an initial MLSS concentration of approximately 3.6 g/L in each photo-reactor. The initial MPs and AMPs concentration in R2 and R3 were roughly 0.1 g/L (dry weight) for a mass ratio to AS of 2.5%. The granulation process can be classified into three phases according to the variations of the indexes (ML(V)SS, SVI_{30}, SVI_{30}/SVI_5 and particle size): initiation, multiplication and stabilization. During the initiation phase (days 0-8), the MLSS concentrations declined from 3.7 g/L to 3.4 g/L (R1), 3.6 g/L (R2) and 3.2 g/L (R3), respectively, which might be subjected to biomass loss associated with the progressive reduction of settling time (Fig. 2a-c). In addition, except for an apparent rise of SVI_{30} in R1 (increased to 56.0 mL/g), the SVI_{30} of R2 and R3 granules decreased to 48.4 mL/g and 47.3 mL/g after 8 days, respectively (Fig. 2d), implying the settling ability of the sludge was improved by dosing the MPs or AMPs. Meanwhile, the mean particle size slightly increased from 82.1 μm to 109.6 μm (R1), 137.7 μm (R2) and 134.0 μm (R3) (Fig. 2e and Fig. S5). The symbiotic growth of algae and bacteria was verified in R3 as the concentration of chlorophyll α increased with operation time (Fig. 2f).

During the multiplication phase (days 8-24), biomass discharge was periodically performed to maintain a relatively stable biomass concentration in all photo-reactors. The MLSS concentrations in R3 was higher than that in R1 and R2, indicating that addition of AMPs enhanced the biomass retention capacity, possibly due to that the algae cell surface properties expedited the bio-flocculation process. Besides, the AMPs exhibited a large specific surface area with high hydrophobicity (due to hydrophobins) that could provide favorable habitats for microorganisms attachment and survival (Liang et al., 2019). The average diameter of the R3 granules underwent a gradual increase to 300 μm and the SVI_{30}/SVI_5 ratio reached 0.87 on day 12 (Fig. 2d,e). Completion of sludge granulation was defined as particle size > 300 μm and SVI_{30}/SVI_5 > 0.8 (Liu and Tay, 2007; Nancharaiah and Reddy, 2018). On the basis of the above criteria, complete granulation of ABGS was achieved within 12 days in R3. Notably, R1 and R2 achieved complete granulation after 28 and 20 days, respectively.

At the stabilization phase (days 24-35), R3 granules exhibited the most excellent sludge characteristics as evidenced by the largest particle size (3.3 mm), the greatest MLSS concentration (2.2 g/L), the highest chlorophyll α content (3.8 mg/L), and the most excellent settleability (SVI_{30}/SVI_5 of 0.99 and SVI_{30} of 53.2 mL/g) (Fig. 2). The stability of sludge is generally expressed as the integrity coefficient (%), with the lower values indicating the better structural stability (Muda et al., 2010). The integrity coefficient (2.74%) of mature ABGS in R3 was much lower than that in R1 and R2 on day 35 (Table S1). In addition, the sludge density of R1 (1.0184 g/mL) was lower than that of R3 (1.0253 g/mL). These results showed that addition of AMPs could effectively accelerate the development of a self-sustaining symbiotic ABGS, and the compact structure deriving from higher biomass retention was contributive to maintain their granular stability.

3.2.2. The observation of ABGS morphology

The brown inoculum sludge gradually turned into a greenish color, and the applied MPs and AMPs started to get smaller during the initiation phase (Fig. 3 and Fig. S6). Many irregular large particles were observed in R1-R3 at the multiplication phase, and they became denser in sphere or ellipse shape at the stabilization phase (Fig. 3a f). High magnification SEM images revealed many protozoa (*Vorticella*) accumulated on the surfaces of R1-R3 granules, signifying a superior effluent quality in the self-sustaining algae-bacterial symbiosis system. No obvious filaments were observed on the mature granule surface of R2 and R3, indicating that the addition of MPs or AMPs did not induce the overgrowth of filamentous bacteria.

Fluorescence microscopic images clearly showed that a spherical

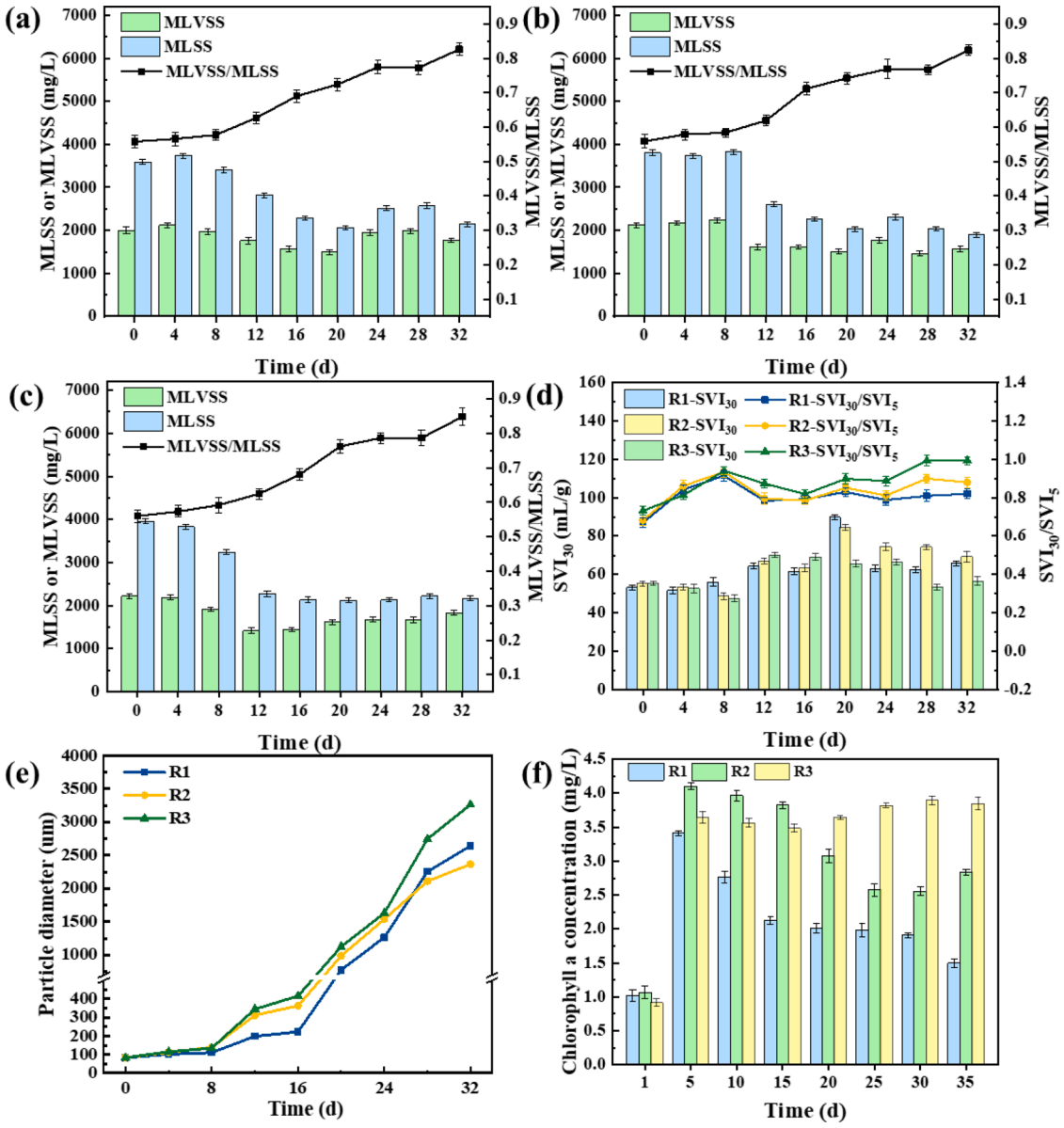

Fig. 2. Changes of sludge characteristics in the three reactors: ML(V)SS in R1-R3 (a c), sludge settling in terms of SVI_{30} and SVI_{30}/SVI_5 (d), mean particle diameter of ABGS (e), and concentration of chlorophyll-α (f). R1: control reactor; R2: MPs reactor; R3: AMPs reactor.

structure of the ABGS was formed with the core of AMPs, in which the mycelium and algae cells were tightly wrapped in the inner part of the granules and the morphological structure of *Chlorella* was integrated (Fig. 3g and Fig. S7). A large number of bacteria (red-stained) adhered onto the surface of hyphae within the granular core of R3, suggesting the role of supporting skeleton played by AMPs (Fig. S7). These observations confirmed that the rapid granulation of ABGS was induced by applying AMPs as the nuclei.

Furthermore, the proteins (green-stained), *α*-polysaccharides (blue-stained) and *β*-polysaccharides (yellow-stained) formed a continuous layer that occupied the central region of the ABGS, constituting the "matrix" of the ABGS. The entwined hyphae in the AMPs provoked the formation of voids and channels within R3 granules (Fig. S7), thus facilitated the mass transfer of substrates and dissolved oxygen, inhibited the filamentous overgrowth and improved the morphological integrity of granules.

3.3. Overall performance, synergistic algal-bacterial reactions and mass balance analysis

3.3.1. Photo-reactor performance

The average COD removal efficiency of R3 (98.6%) was higher than that of R1 (96.4%) and R2 (98.1%) (Fig. 4a). The high MLSS concentration in R3 might provide the reasonable explanation for the high degradation of organic matter. Moreover, MPs have been reported to be efficient in eliminating the contaminants via biosorption and biodegradation (Wang et al., 2010). Similarly, it was considered that the addition of AMPs was beneficial for elevating the COD removal efficiency.

The NH_4^+-N was removed with the overall efficiency approaching 100% in all photo-reactors (data not shown) and negligible NO_2^--N accumulation (< 0.5 mg/L), suggesting the excellent nitrification capability in the ABGS systems. With the extension of operating time, there was an observation of evident declining tendency in the effluent NO_3^--N concentration in R1-R3, which should be responsible for the enhanced TN removal efficiency (Fig. 4c). In comparison, the effluent

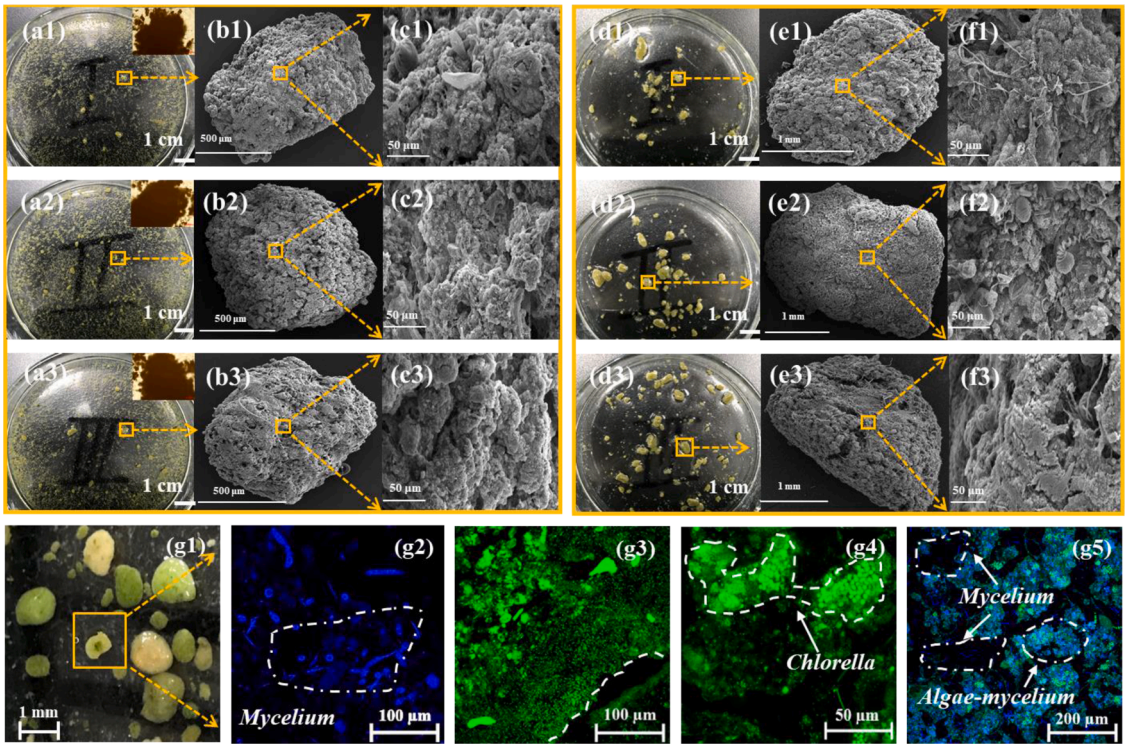

Fig. 3. Digital and SEM images of ABGS collected from R1 (a1 c1 and d1 f1), R2 (a2 c2 and d2 f2), and R3 (a3 c3 and d3 f3) on days 16 and 32, respectively. Fluorescence microscopic images (g2 g5) of algae and mycelium in the interior of R3 granules (g1). The mycelium was stained blue and algal cells were stained green. R1: control reactor; R2: MPs reactor; R3: AMPs reactor.

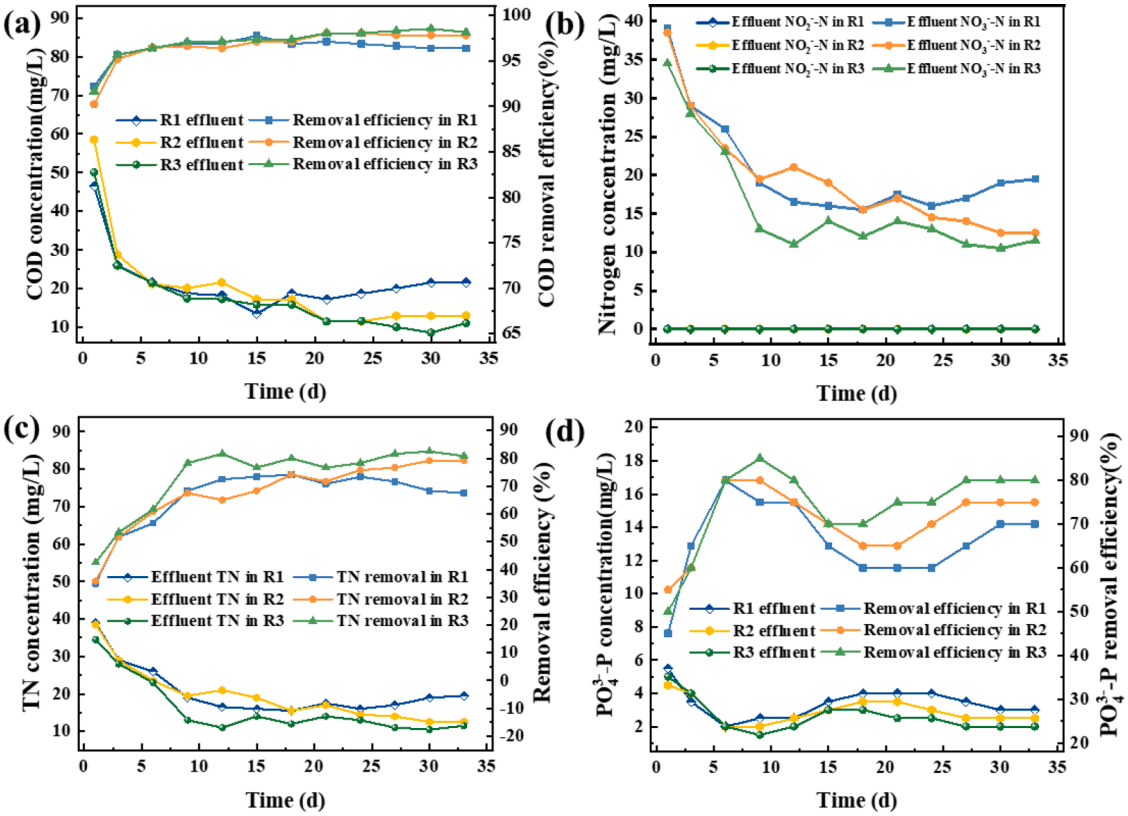

Fig. 4. Variations of COD removal efficiency (a), NO_2^--N and NO_3^--N concentration (b), TN removal efficiency (c), and PO_4^{3-}-P removal efficiency (d). R1: control reactor; R2: MPs reactor; R3: AMPs reactor.

NO_3^--N concentration in R3 (11.5 mg/L) was lower than that in R1 (19.5 mg/L) and R2 (12.5 mg/L) at the end of photo-reactor operation (Fig. 4b). This may be attributable to the expanded granule diameter, whereby the enlarged anaerobic/anoxic region created a more favorable environment for denitrification (Winkler et al., 2013). The average TN removal efficiency (80.8%) obtained in R3 was relatively higher than that of the ABGS cultivated under air-bubbling conditions (averagely 40.3%) (Huang et al., 2020).

Fig. 4d illustrates the PO_4^{3-}-P removal profile in all three photo-reactors. R3 exhibited the most satisfactory performance in PO_4^{3-}-P removal since the removal efficiency averagely exceeded 80.0%. The biological phosphorus removal was the primary mechanism, as the chemical phosphorus removal could be ignored due to the pH below 8.5 in all the photo-reactors (de Godos et al., 2009). As demonstrated earlier, phosphorus present in wastewater in the forms of organic and inorganic phosphorus, both can be effectively utilized by algae cells (He et al., 2018a). Therefore, the improved capability of PO_4^{3-}-P removal in R3 was partially associated with the accumulated algal biomass concentration.

To evaluate the removal pathways of COD and nutrients, typical cycle tests of R1-R3 were performed and compared between the light and dark cycles. The variations in the nutrient concentration followed a parallel pattern during the light and dark cycles in all photo-reactors (Fig. S8). During one cycle, COD and NH_4^+-N were well removed in all three photo-reactors (Fig. S8a-f), suggesting that ABGS had a better capability for COD and NH_4^+-N removal. The PO_4^{3-}-P removal efficiency in the light cycle was better than in the dark cycle in R1-R3 (Fig. S8a c), indicating a certain amount of PO_4^{3-}-P was removed by algal photosynthesis in the light phase. Specifically, the PO_4^{3-}-P concentration gradually increased from 5.0 mg/L to 21.5 mg/L (light cycle) and from 4.0 mg/L to 18.5 mg/L (dark cycle) at the initial 2 h in R3. They gradually declined to 1.0 mg/L (light cycle) and 2.5 mg//L (dark cycle) during the subsequent operating time (2-12 h) (Fig. S8c). This indicated that PO_4^{3-}-P was partially removed by phosphorus accumulating organisms (PAOs) in addition to uptake by algae, which is further investigated in section 3.6.

The above results implied that the addition of AMPs exhibited a promising potential for COD and nutrient removal, likely due to the successful accumulation of algae cells and the enhancement of microbial activities. To investigate the microbial activities, the SOUR, SAUR, and SNUR of the ABGS in all photo-reactors were analyzed (Fig. S9a,b). The maximum SOUR was obtained in R3 (66.2 mg O_2/g MLSS·h), which was higher than that in R1 (61.5 mg O_2/g MLSS·h). Similarly, the SAUR and SNUR of R3 were higher than those in the other two photo-reactors, indicating that the activities of AOB and NOB could be enhanced by applying AMPs as nuclei. The activity of microorganisms can be directly reflected by the content of intracellular adenosine triphosphate (ATP) (Cui et al., 2018). The ATP content of R1 and R2 slightly decreased, respectively, to 4.8 and 5.0 U/mg prot on day 35, while it still maintained at a high level (6.3 U/mg prot) in R3 (Fig. S9c). The reduction in the ATP content implied that a higher fraction of bacteria was inactive or died in R1 and R2 granules, possibly related to the low DO and shear force, whereas the high microbial activity in R3 was contributive to the COD and nutrient removal (Fig. 4). The high microbial activity in R3 was partially owing to the proper mass transfer resistance within the micro-environment (Fig. 3 and Fig. S7) enabled the substrates transportation and created an anoxic zone for denitrification (Geng et al., 2021).

3.3.2. Synergistic algal-bacterial reactions in the ABGS system

In the self-sustaining symbiotic ABGS, O_2 was produced by algae and utilized by aerobic bacteria, i.e. O_2 plays a pivotal role between photosynthetic and heterotrophic reactions. The difference in DO concentration profiles between light and dark phases in a typical cycle (Fig. S8g-i) mirrored closely the coupling of algal photosynthesis and bacterial respiration. The higher DO value during the light cycle was possibly owing to the photosynthesis of algae, which could provide more O_2 to maintain the activity of aerobic bacteria (nitrification and heterotrophic bacteria). It should be noted that, in such a self-sustaining ABGS system, the external aeration was not indispensable, which would save the aeration-associated energy input accounting for approximately 60% of the total energy in the conventional bacteria-based AGS system (Bengtsson et al., 2018).

3.3.3. Mass balance analysis of C, N and P

According to Ji et al., (2021), microbial assimilation is the primary mechanism for C, N, and P removal in an ABGS system. To further ascertain the contribution of algae and bacteria to the removal of C, N and P, the respective synthetic reactions for bacteria and algae were constructed based on the empirical formula, i.e. $CH_{1.4}O_{0.4}N0.2P_{0.017}$ for bacteria and $CH_{1.78}O_{0.36}N_{0.12}P_{0.01}$ for algae (Boelee et al., 2014). The synthetic reactions for bacteria and algae are described in Eq. (2) and Eq. (3), respectively.

Bacterial assimilation reaction with acetate as the organic carbon source:

$$CH_3COO^- + 0.88O_2 + 0.22NH_4^+ + 0.019H_2PO_4^- + 0.8H^+ = 0.91CO_2 + 1.6H_2O + 1.1CH_{1.4}N_{0.2}O_{0.4}P_{0.017} \quad (2)$$

Algal assimilation reaction with CO_2 as carbon source:

$$CO_2 + 0.12NH_4^+ + 0.01H_2PO_4^- + 0.69H_2O = 1.19O_2 + 0.11H^+ + CH_{1.78}N_{0.12}O_{0.36}P_{0.01} \quad (3)$$

Therefore, the mass ratio (f) of removed carbon to nitrogen can be estimated from Eq. (4), i.e.

$$f = \sum\left(C_{COD_{inf.}} - C_{COD_{eff.}}\right)/1.1 \times 2M_C \Big/ M_{AC^-} \Big/ \sum\left(C_{NH_4^+-N_{inf.}} - C_{NH_4^+-N_{eff.}}\right) \quad (4)$$

where $C_{COD_{inf.}}$ and $C_{NH_4^+-N_{inf.}}$ are influent COD concentration and NH_4^+-N concentration, respectively; $C_{COD_{eff.}}$ and $C_{NH_4^+-N_{eff.}}$ are effluent COD concentration and NH_4^+-N concentration, respectively; while M_C and M_{AC^-} are the molecular weights of carbon and Ac^-, respectively. In addition, the coefficient 1.1 is the conversion ratio of Ac^- to COD.

Fig. 5 shows that C, N and P were majorly removed by bacterial metabolism, which was consistent with Ji et al., (2020). Furthermore, 34.6% of C, 17.0% of N, 10.0% of P were removed by algae in R3 system, which were higher than those in R1 and R2. Some algae species (especially green algae) are able to take up nutrients (nitrogen and phosphorus) as energy sources for synthesizing their own cellular substances (Lee et al., 2015). The higher retention of algae biomass (chlorophyll α content of 3.8 mg/L) in R3 because of the efficient flocculation by MPs could also contribute to the efficient nutrient removal.

3.4. EPS production of ABGS

3.4.1. Analysis of PN and PS content

EPS secreted by microorganisms play a key role in the sludge granulation and the structural stability of ABGS (Shi and Liu, 2021). With the progress of granulation, the PN content gradually increased to the maximal value of 44.9 mg/g SS (R1), 46.3 mg/g SS (R2), and 51.1 mg/g SS (R3), which was, respectively, 3.1, 3.2, and 3.6 folds higher than that of the activated sludge (Fig. 6a c). Notably, the variation tendency of PN/PS ratio (over the range of 1.35 to 4.03) was analogous to that of the PN content (Fig. 6a c), with observation of no considerable fluctuation in PS content in all photo-reactors throughout the whole process. This is in line with a previous study where the granulation was positively affected by PN especially for the primary stage (He et al., 2018b).

At a later stage of the experiment, the PN content dramatically decreased in R1 and slightly decreased in R2, while it remained steady in

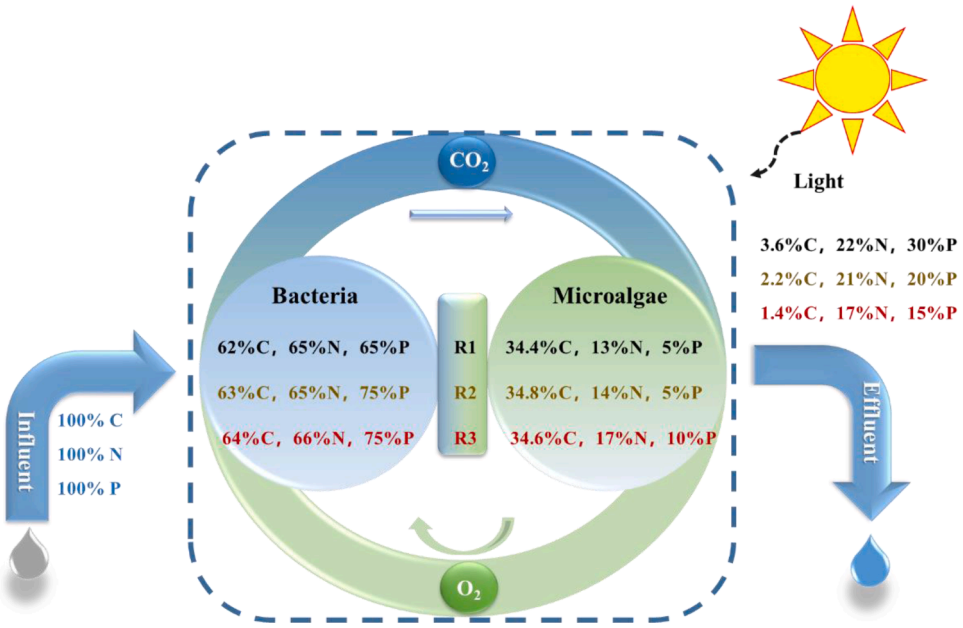

Fig. 5. Mass flows of carbon, nitrogen and phosphorus of the ABGS in R1-R3. R1: control reactor; R2: MPs reactor; R3: AMPs reactor.

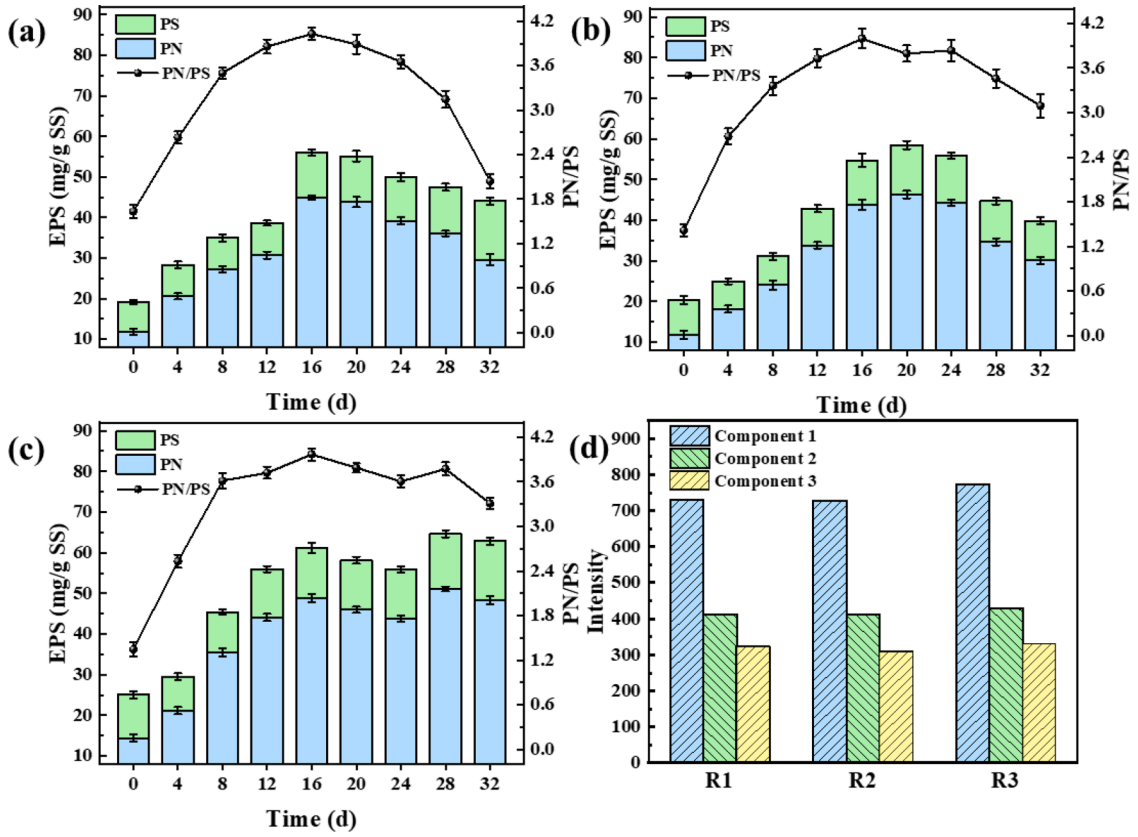

Fig. 6. Changes of EPS concentrations and PN/PS ratios of the ABGS in R1-R3 (a-c). Peak intensity variations of the different components identified by PARAFAC in R1-R3 (d). R1: control reactor; R2: MPs reactor; R3: AMPs reactor.

R3. Finally, the PN content followed an increasing order: R1 (29.6 mg/g SS) < R2 (34.7 mg/g SS) < R3 (48.3 mg/g SS). A similar pattern was observed that the addition of MPs could stimulate bacteria to produce more PN (Geng et al., 2020). PN are relatively hydrophobic substances, and the high level of relative hydrophobicity contributes to the decrease of the Gibbs free energy, thus facilitating the microorganisms to aggregate together and enhancing the stability of the self-sustaining symbiotic ABGS system (Zhang et al., 2020a).

3.4.2. *Functional groups and fluorescent components of EPS*

FTIR spectrometry was adopted to identify the functional groups of EPS samples obtained from the ABGS and inoculum sludge (Fig. S10).

The intensities of two absorption peaks appeared at 3440 cm^{-1} (associated with the polysaccharide-OH stretching vibration) and 1646 cm^{-1} (associated with the C=O bond (amide I) in the protein primary structure) were observed to be strengthened in the ABGS samples compared to the inoculum sludge, which was consistent with the improvement of PN content (Fig. 6a-c). In addition, the peak at 1096 cm^{-1} (or 1033 cm^{-1}) attributing to polysaccharide C=O stretching vibration existed in all EPS samples (Lotti et al., 2019). In comparison, the intensity of this absorption peak in the ABGS was obviously lower than the inoculum sludge. This implied that polysaccharides were not the active agents to promote microbial aggregation.

3D-EEM fluorescence spectroscopy was employed to identify the fluorescent components in the EPS (Fig. S11). Due to the complex compositions of EPS, the fluorescence spectra seriously overlapped in Fig. S11. Parallel factor (PARAFAC) analysis was, therefore, performed to separate the EEM spectra into independent components (Ishii and Boyer, 2012). Three components were identified as Component 1, Component 2 and Component 3 (Table 1). Component 1, with two peaks at Ex/Em of 220-230/325-375 nm and 250-300/325-375 nm, represent the tryptophan and aromatic protein-like substances. Component 2, with Ex/Em at 200-230/350-450 nm and 250-300/350-450 nm, was classified as fulvic-like and humic-like substances. Component 3, with Ex/Em at 200-230/300-325 nm, was identified as protein-like substances, mainly tyrosine substances (Luo et al., 2014).

Notably, the FI value of component 1 in R3 (772.2) was obviously higher than that in R1 and R2, while no significant difference was obtained between R1 (731.4) and R2 (728.5). For components 2 and 3, there was no obvious difference among the three photo-reactors (Fig. 6d). Therefore, it was considered that applying AMPs as nuclei enhanced the sludge granulation by stimulating the secretion of tryptophan and aromatic protein substances.

3.5. Analysis of surface free energy of ABGS

3.5.1. Electronegativity and hydrophobicity

The zeta potential of the activated sludge was -14.00 mV, and it gradually increased along with the granulation process (Table S2). At the end of the photo-reactor operation, the highest zeta potential (-11.30 mV) was obtained in R3, indicating the electrostatic repulsion between the microorganisms was greatly weakened, which was conducive to their mutual aggregation (Liu et al., 2007).

Furthermore, the contact angles of all the sludge samples against water, formamide and diiodomethane exhibited distinct increases after complete granulation (Table S2). Notably, the contact angle between R3 granules and water clearly increased (87.71°). Hydrophobicity can be considered to be dominant when the contact angle between the microbial cell surface and water is higher than 65° (Liu et al., 2008). These results indicated that the hydrophobicity of the sludge surface was improved by applying AMPs as nuclei in a self-sustaining symbiotic ABGS system. Cell hydrophobicity is the initial driving force that promotes granular sludge formation and is a crucial factor in bacterial aggregation (Liu and Tay, 2004). As described earlier, the enhancement of

Table 2
Surface energetic parameters and surface free energy of the inoculum sludge and ABGS taken from R1-R3 (on day 32).

Reactor	Surface energetic parameters (mJ/m^2)					Surface free energy (mJ/m^2)
	γ^{LW}	γ^{+}	γ^{-}	γ^{AB}	γ^{TOT}	ΔG_{adh}
Inoculum sludge	37.52	0.64	6.85	4.18	41.70	-44.26
R1	36.66	1.21	1.89	3.02	39.68	-60.83
R2	36.59	1.25	0.89	2.11	38.70	-67.34
R3	36.43	0.01	3.26	0.42	36.85	-69.56

Table 1
Component labels, peak locations, corresponding EEMs and spectral loadings for different components.

Component label	Approximate EEM location	EEM	Spectral loadings
1	Em: 325-375 Ex: 220-230/250-300	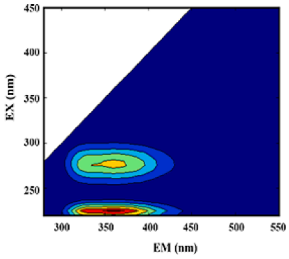	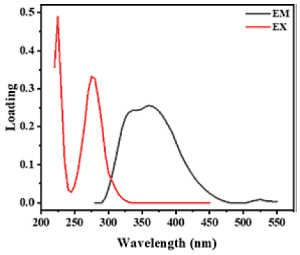
2	Em: 350-450 Ex: 200-230/250-300	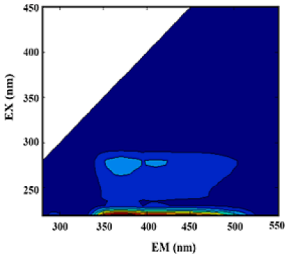	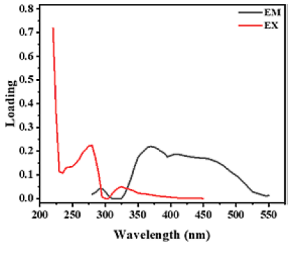
3	Em: 300-325 Ex: 200-230	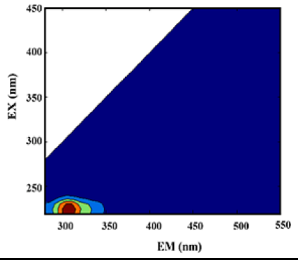	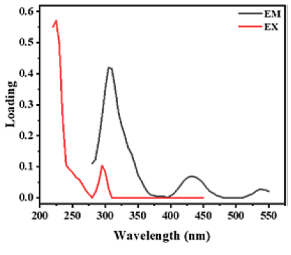

hydrophobicity on the cell surface was beneficial for promoting the microbial aggregation and subsequently forming a more compact three-dimensional granular structure (Adav et al., 2008).

3.5.2. Surface thermodynamic analysis based on XDLVO theory

The free energy values and the parameters related to the surface thermodynamics of sludge samples were calculated according to the formula of the surface thermodynamic analysis, and the results are shown in Table 2. The magnitude of the interfacial free energy (ΔG_{adh}) can be used to determine the hydrophobicity of the sludge surface (Brant and Childress, 2002). Here, the ΔG_{adh} values of R3 (-69.56 mJ/m^2) was lower than that of R1 (-60.83 mJ/m^2) and R2 (-67.34 mJ/m^2) granules. According to the thermodynamic theory, adhesion between microorganisms is more prone to occur if the ΔG_{adh} value is lower (Liu et al., 2008). Therefore, it was demonstrated that the addition of AMPs positively modified the thermodynamic characteristics of the sludge surface, and the hydrophobicity of the sludge surface was improved, which is consistent with the contact angles results (Table S2).

Herein, the XDLVO theory was further employed to reveal the inherent mechanism of bacterial aggregation. The potential energy barrier existed on all the total potential energy curves of R1-R3 (Fig. 7). Aggregation could occur when microorganisms had enough energy to surpass this potential energy barrier (Liu et al., 2008). Besides, the lower energy barrier indicated that lower energy was required by the microorganisms to aggregate. The total potential energy curves showed that R1 and R2 reached the energy barrier of 138.98 kT and 109.64 kT at 5.50 nm and 5.65 nm, respectively, while R3 reached the energy barrier (89.93 KT) at 5.75 nm, indicating that R3 had the lowest energy barrier and the strongest capacity of microbial aggregation.

3.6. Community structure dynamics of bacteria, algae and fungus

In contrast to the inoculum sludge, the ABGS samples had a higher Simpson index and lower Shannon index, indicating that the bacterial diversity of the microbial population decreased in the ABGS system (Table S3). In addition, the inoculum sludge exhibited a higher Ace index (1000) and Chao index (1007) compared to ABGS samples, demonstrating that the microbial population in the inoculum sludge was more abundant. This observation is consistent with Guo et al., (2019), who suggested that the richness and diversity of microorganisms decreased during the granulation.

As the granulation progressed, the phylum *Actinobacteriota* sharply dropped to below 0.21% in all three photo-reactors. Nevertheless, the relative abundance of the phylum *Proteobacteria* was dramatically improved during the photo-granulation, especially in R3 (62.68%), which was 3.7 folds higher than that in the inoculum sludge (16.91%) (Fig. 8a). Lots of evidence confirmed that most of the PAOs belong to the phylum *Proteobacteria* (Zhang et al., 2012). The heat-map showed that the dominant genus in all ABGS samples were significantly different from the inoculum sludge (Fig. 8e). To be specific, the relative abundance of the genus *Neomegalonema* affiliating to the phylum *Proteobacteria* significantly increased to 43.82% (R1), 20.71% (R2), and 46.11% (R3) (Fig. 8b). The N and P removal efficiencies and EPS content were found to be positively correlated with *Neomegalonema* (Fig. 8f). This bacterial genus is well-known for taking up organic and nitrogenous substances, and it is also a PAO and EPS producer (Cruz et al., 2022; Ramos et al., 2015). Therefore, it was inferred that the superior removal efficiencies of COD, NH_4^+-N and PO_4^{3-}-P as well as the higher EPS content in R3 could be partially ascribed to the proliferation of this genus.

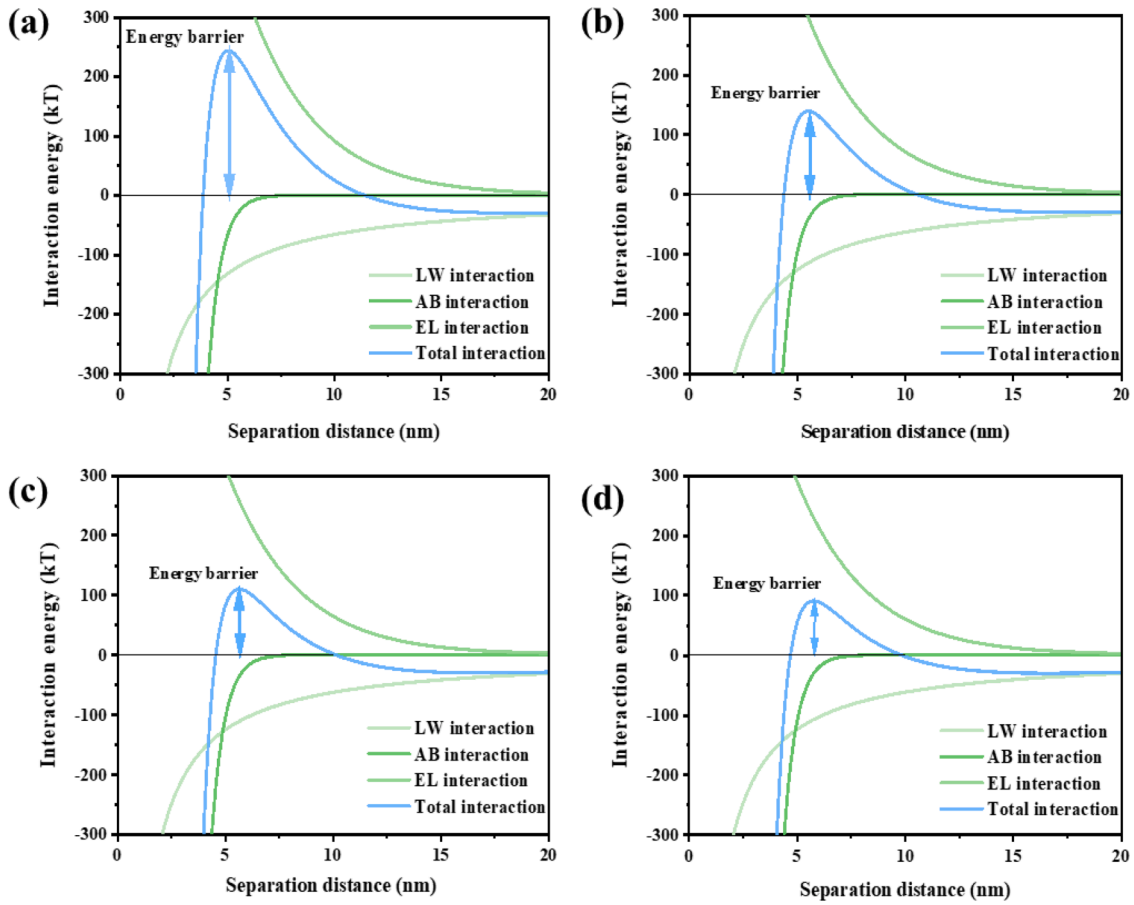

Fig. 7. XDLVO curves of the inoculum sludge (a) and ABGS in R1-R3 (b d). R1: control reactor; R2: MPs reactor; R3: AMPs reactor.

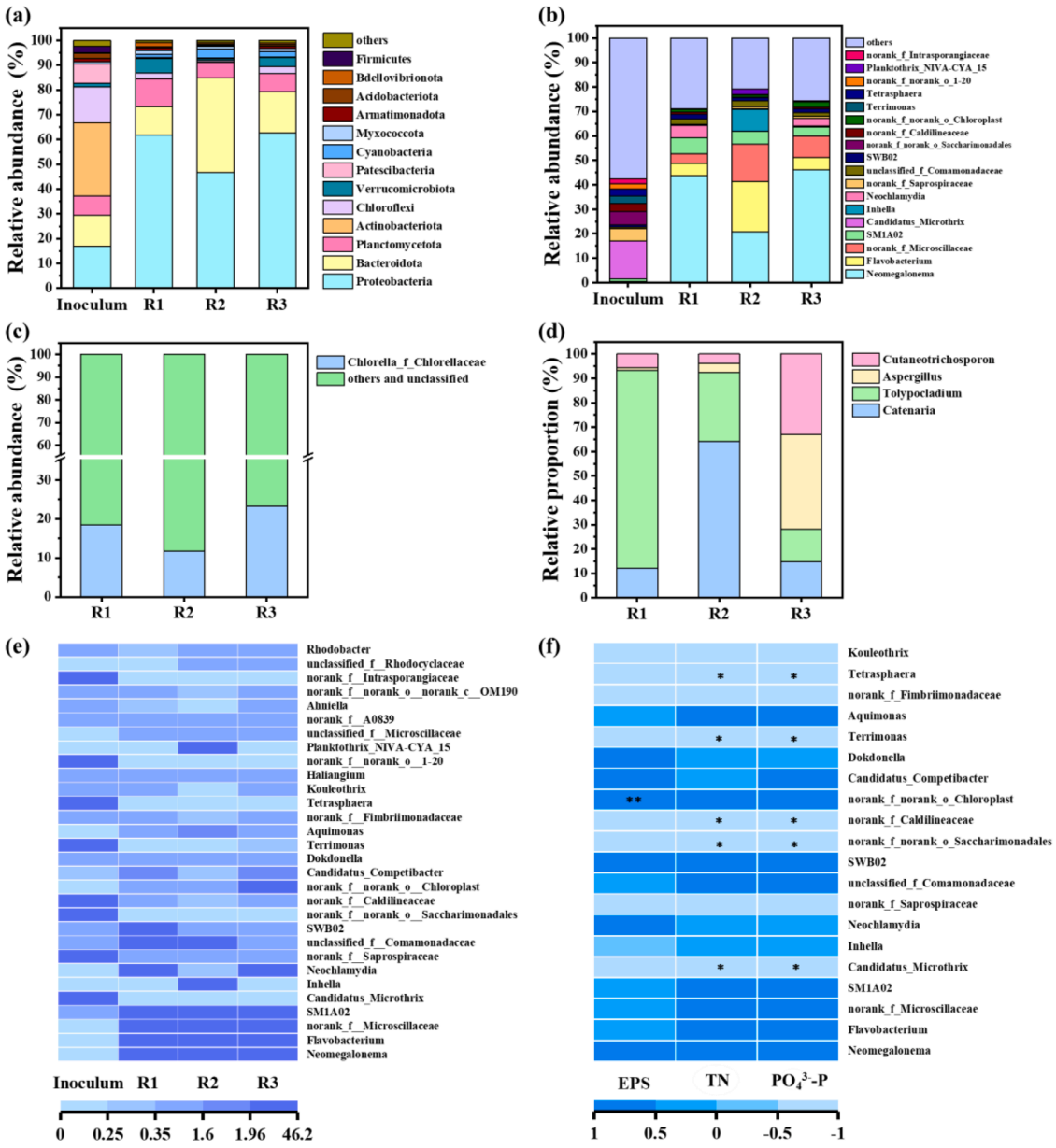

Fig. 8. Bacterial communities of the inoculum sludge and R1 R3 granules at phylum (a) and genus (b) level. The relative abundance of the identified algal genera in R1 R3 granules (c) and the relative proportion of identified fungi in R1 R3 granules at genus level (d). Heat-map of the identified bacteria genus in the inoculum sludge and R1 R3 granules (e). The relationship between the top 20 genus and EPS content and N, P removal (f). * denotes $p < 0.05$, ** denotes $p < 0.01$.

Furthermore, the relative abundance of the genus *Flavobacterium* from the phylum *Bacteroidota* gradually increased to 5.12% in R3, and exhibited a positive relationship with the EPS production, as well as nitrogen and phosphorus removal efficiency (Fig. 8f). This is agree with a previous work which indicated that *Flavobacterium* was an EPS secreting bacterium with strong self-agglomeration ability (Liu et al., 2017). Besides, as a denitrifying phosphate accumulating organism (DPAO), *Flavobacterium* could assist in simultaneous removal of nitrogen and phosphate (Sengar et al., 2018). Thereby, the higher abundance of *Flavobacterium* may have supported the nutrient removal in R3. For the inoculum sludge, the genus *Candidatus_Microthrix* is the most abundant bacterium (15.48%), however, it almost disappeared in the ABGS. As reported before, the filamentous bacteria *Candidatus_Microthrix* is a filamentous bacteria, which prefers to dominate in the loosely structured sludge (Blackall et al., 1996). This corresponded well to the observation that there were no visible filaments attached on the surface of R3 granules (Fig. 3).

As for the algal community, the algae *Chlorella* was identified in all ABGS samples because of the targeted control (Fig. 8c). Comparatively, the relative abundance of *Chlorella_f_Chlorellaceae* in R3 (23.25%) was higher than that of R1 (18.52%) and R2 (11.68%) sludge, indicating that algal cells were effectively enriched in R3. *Chlorella* is capable of assimilating N and P from wastewater into cellular components, such as phospholipids, nucleic acids and nucleotides during the growth process, which favors the nutrients removal from wastewater (Mahapatra et al., 2013). Therefore, it was suggested that the addition of AMPs could retain the targeted algae in the system, which was beneficial for enhancing the nutrient removal and establishing the favorable symbiosis between bacteria and algae.

Fig. 8d shows that the most dominant fungi in the ABGS were *Tolypocladium* (R1), *Catenaria* (R2), and *Aspergillus* (R3), respectively. Among the classified fungi, the genus *Aspergillus* accounted for 38.76% in R3 and was distinctly higher than that in R1 (0.96%) and R2 (3.76%). Thereby, the addition of MPs could not only effectively retain the

Aspergillus, but the growth and bioactivity of *Aspergillus* could be well maintained in the photo-bioreactor via the addition of AMPs.

3.7. Mechanisms analysis and practical implications of this study

In this study, the development process of ABGS induced by AMPs as nuclei was analyzed to further unravel the internal enhancement mechanisms. Firstly, many flocs attached onto the surface of the AMPs on day 5, implying the initial formation of AMPs-based granules (Fig. S4). However, the young AMPs-based granules appeared to be destabilized and broke into several fragments on day 8, as evidenced by the morphological observation of the granules (Fig. S6). Afterwards, the fragments of granules acted as nuclei and induced the formation of compact granules (Fig. 3g and Fig. S7). This result was consistent with Wang et al., (2014) and Geng et al., (2020), who reported that the fragments resulting from the granular disintegration could serve as nuclei for the re-production of granules.

AMPs formed by combining MPs with algal cells secreted a large amount of EPS (detailed analysis see Fig. S12 and Text S3), which was conducive to accelerate the granulation process (Wang et al., 2019). With the enhancement of bacterial collisions and EPS secretion, the particle diameter was further enlarged and thus provided sufficient ecological niches for the growth of the genus *Neomegalonema, Flavobacterium* and *norank_f_Microscillaceae*. These bacteria are capable of degrading organic and nitrogenous substances. In addition, the inoculated algae were effectively enriched in the system and a good symbiotic relationship between bacteria and algae was established. Consequently, satisfactory nitrogen and phosphorus removal (averagely 100.0% and 80.8%, respectively) from the wastewater was realized.

The analysis of the surface free energy of the ABGS further revealed that the addition of AMPs could provide more energy to overcome the electrostatic repulsive forces between the cells (ΔG_{adh} values of -69.56 mJ/m^2), thereby inducing the microbial aggregation. Notably, the mature ABGS inhibited the overgrowth of filamentous bacteria, which was beneficial for maintaining the long-term stability of the ABGS systems (Fig. 8). In a nutshell, this study showed that applying AMPs as the primary nuclei significantly accelerated the development of ABGS.

It is worth emphasizing that except for rapid start-up of ABGS system and efficient nutrient removal, this novel strategy is also promising in the following aspects. a) Rapid formation and easy separation of AMPs. Based on the co-pelletization strategy, the algal cells (*Chlorella*) were entrapped in the MPs of *Aspergillus* within 12 h under the optimized conditions. The formed AMPs (1-2 mm in diameter) with excellent settling capability could be easily separated from the culture media merely relying on gravity sedimentation. b) Low dosage amount of AMPs. In addition, experimental results indicated that the optimal dry mass ratio of AMPs and activated sludge was as low as 2.5%, much lower than the dosage amount of MPs (up to 60%, w/w) as carriers for accelerating the aerobic sludge granulation (Geng et al., 2021), indicating that this strategy was economically competitive and thereby could be envisaged for large-scale application. c) Great potential for resource recovery. Most of the nutrients in the wastewater were removed via bacterial and algal assimilations during the photo-granulation process (Fig. 5), i.e. they were concentrated in the ABGS biomass. Besides, the fungal genus *Aspergillus*, which can produce enzymes such as laccase and protease (Cabaleiro et al., 2002), and a cyclosporin-producing fungus *Tolypocladium* (Aarnio and Agathos, 1989) were also accumulated in the ABGS. Therefore, the ABGS biomass has a broad prospect to be a potential resource recovery factory in the forms of biodiesel, fertilizers, pharmaceuticals, etc.

Despite of the aforementioned advantages, further research should be carried out at pilot or full scale facilities to provide data from practical applications and prolong the operational process to verify the long-term effects of implementing this strategy. On the road to advance this promising technology towards engineering applications, significant efforts are required on a paradigm shift of the ABGS system from current single-functionality (nutrient removal) toward multiple-functionality (wastewater treatment-energy production-resource recovery) for maximizing the environmental sustainability and economic viability.

4. Conclusions

A novel strategy by using AMPs as nuclei was proposed with the purpose to accelerate the development of a self-sustaining symbiotic ABGS. The results showed that the ABGS was rapidly developed within 12 days, with large particle size, compact structure and excellent settling property, high bioactivity, and satisfactory nutrient removal efficiency. The fungus (*Aspergillus*) with the targeted algae (*Chlorella*) acted as the granule nuclei, the reinforced secretion of tryptophan and aromatic protein as well as the enrichment of functional bacteria (such as *Neomegalonema* and *Flavobacterium*) contributed to the rapid granulation of ABGS. The surface free energy of ABGS indicated that the repulsive barrier between microorganisms was significantly decreased, which was the inherent mechanism for the readily bacterial aggregation. Overall, this study provided a cost-efficient and practically feasible approach to accelerate the development of a self-sustaining symbiotic ABGS.

Declaration of Competing Interest

The authors declare that they have no known competing financial interests or personal relationships that could have appeared to influence the work reported in this paper.

Acknowledgements

The authors acknowledge National Natural Science Foundation of China (Grant no. 52000014 and 51978098) and China Postdoctoral Science Foundation (Grant no. 2020M683249 and 2021T140781) for their financial support.

Supplementary materials

Supplementary material associated with this article can be found, in the online version, at doi:10.1016/j.watres.2022.118210.

References

Aarnio, T.H., Agathos, S.N., 1989. Production of extracellular enzymes and cyclosporin by tolypocladium inflatum and morphologically related fungi. Biotechnol. Lett 11 (11), 759–764. https://doi.org/10.1007/bf01026092.

Adav, S.S., Lee, D.J., Show, K.Y., Tay, J.H., 2008. Aerobic granular sludge: recent advances. Biotechnol. Adv. 26 (5), 411–423. https://doi.org/10.1016/j.biotechadv.2008.05.002.

Ahmad, J.S.M., Cai, W., Zhao, Z., Zhang, Z., Shimizu, K., Lei, Z., Lee, D.J., 2017. Stability of algal-bacterial granules in continuous-flow reactors to treat varying strength domestic wastewater. Bioresour. Technol. 244, 225–233. https://doi.org/10.1016/j.biortech.2017.07.134.

APHA, 2005. Standard methods for the examination of water and wastewater.

Bengtsson, S., de Blois, M., Wilén, B.-M., Gustavsson, D., 2018. Treatment of municipal wastewater with aerobic granular sludge. Crit. Rev. Environ. Sci. Technol. 48 (2), 119–166. https://doi.org/10.1080/10643389.2018.1439653.

Blackall, L.L., Stratton, H., Bradford, D., delDot, T., Sjorup, C., Seviour, E.M., Seviour, R. J., 1996. *Candidatus Microthrix parvicella*'', a filamentous bacterium from activated sludge sewage treatment plants. Int. J. Syst. Bacteriol. 46 (1), 344–346. https://doi.org/10.1099/00207713-46-1-344.

Boelee, N.C., Temmink, H., Janssen, M., Buisman, C.J.N., Wijffels, R.H., 2014. Balancing the organic load and light supply in symbiotic microalgal-bacterial biofilm reactors treating synthetic municipal wastewater. Ecol. Eng. 64, 213–221. https://doi.org/10.1016/j.ecoleng.2013.12.035.

Brant, J.A., Childress, A.E., 2002. Assessing short-range membrane-colloid interactions using surface energetics. J. Membr. Sci. 203 (1-2), 257–273. https://doi.org/10.1016/s0376-7388(02)00014-5.

Cabaleiro, D.R., Rodriguez-Couto, S., Sanroman, A., Longo, M.A., 2002. Comparison between the protease production ability of ligninolytic fungi cultivated in solid state media. Process Biochem. 37 (9), 1017–1023. https://doi.org/10.1016/s0032-9592(01)00307-7.

Chen, J., Leng, L., Ye, C., Lu, Q., Addy, M., Wang, J., Liu, J., Chen, P., Ruan, R., Zhou, W., 2018. A comparative study between fungal pellet- and spore-assisted microalgae

harvesting methods for algae bioflocculation. Bioresour. Technol. 259, 181–190. https://doi.org/10.1016/j.biortech.2018.03.040.
Cruz, R.A.P., Oehmen, A., Reis, M.A.M., 2022. The impact of biomass withdrawal strategy on the biomass selection and polyhydroxyalkanoates accumulation of mixed microbial cultures. New Biotechnol. 66, 8–15. https://doi.org/10.1016/j.nbt.2021.08.004.
Cui, X., Huo, M., Chen, C., Yu, Z., Zhou, C., Li, A., Qiao, B., Zhou, D., Crittenden, J.C., 2018. Low concentrations of Al (III) accelerate the formation of biofilm: multiple effects of hormesis and flocculation. Sci. Total Environ. 634, 516–524. https://doi.org/10.1016/j.scitotenv.2018.03.376.
de Godos, I., Blanco, S., Garcia-Encina, P.A., Becares, E., Munoz, R., 2009. Long-term operation of high rate algal ponds for the bioremediation of piggery wastewaters at high loading rates. Bioresour. Technol. 100 (19), 4332–4339. https://doi.org/10.1016/j.biortech.2009.04.016.
Dubois, M., Gilles, K.A., Hamilton, J.K., Rebers, P.A., Smith, F., 1956. Colorimetric method for determination of sugars and related substances. Anal. Chem. 28 (3), 350–356. https://doi.org/10.1021/ac60111a017.
Fomina, M., Gadd, G.M., 2002. Influence of clay minerals on the morphology of fungal pellets. Mycol. Res. 106, 107–117. https://doi.org/10.1017/s0953756201004786.
Gardes, M., Bruns, T.D., 1993. ITS primers with enhanced specificity for Basidiomycetes-application to the identification of mycorrhizae and rusts. Mol. Ecol. 2 (2), 113–118. https://doi.org/10.1111/j.1365-294X.1993.tb00005.x.
Geng, M., Ma, F., Guo, H., Su, D., 2020. Enhanced aerobic sludge granulation in a sequencing batch reactor (SBR) by applying mycelial pellets. J. Cleaner Prod. 274, 123037 https://doi.org/10.1016/j.jclepro.2020.123037.
Geng, M., You, S., Guo, H., Ma, F., Xiao, X., Zhang, J., 2021. Impact of fungal pellets dosage on long-term stability of aerobic granular sludge. Bioresour. Technol. 332, 125106 https://doi.org/10.1016/j.biortech.2021.125106.
Guo, Y., Zhang, B., Zhang, Z., Shi, W., Zhang, R., Cheng, J., Li, W., Cui, F., 2019. Enhanced aerobic granulation by applying the low-intensity direct current electric field via reactive iron anode. Water Res. 149, 159–168. https://doi.org/10.1016/j.watres.2018.10.095.
He, Q., Chen, L., Zhang, S., Chen, R., Wang, H., Zhang, W., Song, J., 2018a. Natural sunlight induced rapid formation of water-born algal-bacterial granules in an aerobic bacterial granular photo-sequencing batch reactor. J. Hazard. Mater. 359, 222–230. https://doi.org/10.1016/j.jhazmat.2018.07.051.
He, Q., Song, Q., Zhang, S., Zhang, W., Wang, H., 2018b. Simultaneous nitrification, denitrification and phosphorus removal in an aerobic granular sequencing batch reactor with mixed carbon sources: reactor performance, extracellular polymeric substances and microbial successions. Chem. Eng. J. 331, 841–849. https://doi.org/10.1016/j.cej.2017.09.060.
Huang, W., Li, B., Zhang, C., Zhang, Z., Lei, Z., Lu, B., Zhou, B., 2015. Effect of algae growth on aerobic granulation and nutrients removal from synthetic wastewater by using sequencing batch reactors. Bioresour. Technol. 179, 187–192. https://doi.org/10.1016/j.biortech.2014.12.024.
Huang, W., Liu, D., Huang, W., Cai, W., Zhang, Z., Lei, Z., 2020. Achieving partial nitrification and high lipid production in an algal-bacterial granule system when treating low COD/NH_4^+-N wastewater. Chemosphere 248, 126106. https://doi.org/10.1016/j.chemosphere.2020.126106.
Ishii, S.K., Boyer, T.H., 2012. Behavior of reoccurring PARAFAC components in fluorescent dissolved organic matter in natural and engineered systems: a critical review. Environ. Sci. Technol. 46 (4), 2006–2017. https://doi.org/10.1021/es2043504.
Ji, B., Liu, C., 2022. CO_2 improves the microalgal-bacterial granular sludge towards carbon-negative wastewater treatment. Water Res. 208, 117865 https://doi.org/10.1016/j.watres.2021.117865.
Ji, B., Zhang, M., Gu, J., Ma, Y., Liu, Y., 2020. A self-sustaining synergetic microalgal-bacterial granular sludge process towards energy-efficient and environmentally sustainable municipal wastewater treatment. Water Res. 179, 115884 https://doi.org/10.1016/j.watres.2020.115884.
Ji, B., Zhu, L., Wang, S., Liu, Y., 2021. Temperature-effect on the performance of non-aerated microalgal-bacterial granular sludge process in municipal wastewater treatment. J. Environ. Manage. 282, 111955 https://doi.org/10.1016/j.jenvman.2021.111955.
Jiang, B., Liu, Y., 2012. Roles of ATP-dependent N-acylhomoserine lactones (AHLs) and extracellular polymeric substances (EPSs) in aerobic granulation. Chemosphere 88 (9), 1058–1064. https://doi.org/10.1016/j.chemosphere.2012.04.059.
Lahlali, R., Hijri, M., 2010. Screening, identification and evaluation of potential biocontrol fungal endophytes against *Rhizoctonia solani* AG3 on potato plants. FEMS Microbiol. Lett. 311 (2), 152–159. https://doi.org/10.1111/j.1574-6968.2010.02084.x.
Lee, C.S., Lee, S.-A., Ko, S.-R., Oh, H.-M., Ahn, C.-Y., 2015. Effects of photoperiod on nutrient removal, biomass production, and algal-bacterial population dynamics in lab-scale photobioreactors treating municipal wastewater. Water Res. 68, 680–691. https://doi.org/10.1016/j.watres.2014.10.029.
Li, L., Liang, T., Liu, W., Liu, Y., Ma, F., 2020. A comprehensive review of the mycelial pellet: research status, applications, and future prospects. Ind. Eng. Chem. Res. 59 (39), 16911–16922. https://doi.org/10.1021/acs.iecr.0c01325.
Li, Y., Xu, Y., Liu, L., Li, P., Yan, Y., Chen, T., Zheng, T., Wang, H., 2017. Flocculation mechanism of *Aspergillus niger* on harvesting of *Chlorella vulgaris* biomass. Algal Res. 25, 402–412. https://doi.org/10.1016/j.algal.2017.06.001.
Liang, Z., Tu, Q., Su, X., Yang, X., Chen, J., Chen, Y., Li, H., Liu, C., He, Q., 2019. Formation, extracellular polymeric substances, and structural stability of aerobic granules enhanced by granular activated carbon. Environ. Sci. Pollut. Res. Int. 26 (6), 6123–6132. https://doi.org/10.1007/s11356-018-04101-1.
Liu, H., Zhu, L., Tian, X., Yin, Y., 2017. Seasonal variation of bacterial community in biological aerated filter for ammonia removal in drinking water treatment. Water Res. 123, 668–677. https://doi.org/10.1016/j.watres.2017.07.018.
Liu, L., Hong, Y., Ye, X., Wei, L., Liao, J., Huang, X., Liu, C., 2018. Biodiesel production from microbial granules in sequencing batch reactor. Bioresour. Technol. 249, 908–915. https://doi.org/10.1016/j.biortech.2017.10.105.
Liu, X.M., Sheng, G.P., Q, Y.H., 2007. DLVO approach to the flocculability of a photosynthetic H_2-producing bacterium, *Rhodopseudomonas acidophila*. Environ. Sci. Technol 41 (13), 4620–4625. https://doi.org/10.1021/es070107n.
Liu, X.M., Sheng, G.P., Wang, J., Yu, H.Q., 2008. Quantifying the surface characteristics and flocculability of *Ralstonia eutropha*. Appl. Microbiol. Biotechnol. 79 (2), 187–194. https://doi.org/10.1007/s00253-008-1426-1.
Liu, Y.-Q., Tay, J.-H., 2007. Characteristics and stability of aerobic granules cultivated with different starvation time. Appl. Microbiol. Biotechnol. 75 (1), 205–210. https://doi.org/10.1007/s00253-006-0797-4.
Liu, Y., Tay, J.H., 2004. State of the art of biogranulation technology for wastewater treatment. Biotechn. Adv. 22 (7), 533–563. https://doi.org/10.1016/j.biotechadv.2004.05.001.
Lotti, T., Carretti, E., Berti, D., Martina, M.R., Lubello, C., Malpei, F., 2019. Extraction, recovery and characterization of structural extracellular polymeric substances from anammox granular sludge. J. Environ. Manage. 236, 649–656. https://doi.org/10.1016/j.jenvman.2019.01.054.
Lu, Y.Z., Ding, Z.W., Ding, J., Fu, L., Zeng, R.J., 2015. Design and evaluation of universal 16S rRNA gene primers for high-throughput sequencing to simultaneously detect DAMO microbes and anammox bacteria. Water Res. 87, 385–394. https://doi.org/10.1016/j.watres.2015.09.042.
Luo, J., Hao, T., Wei, L., Mackey, H.R., Lin, Z., Chen, G.-H., 2014. Impact of influent COD/N ratio on disintegration of aerobic granular sludge. Water Res. 62, 127–135. https://doi.org/10.1016/j.watres.2014.05.037.
Mahapatra, D.M., Chanakya, H.N., Ramachandra, T.V., 2013. *Euglena* sp as a suitable source of lipids for potential use as biofuel and sustainable wastewater treatment. J. Appl. Phycol. 25 (3), 855–865. https://doi.org/10.1007/s10811-013-9979-5.
Meng, F., Liu, D., Huang, W., Lei, Z., Zhang, Z., 2019a. Effect of salinity on granulation, performance and lipid accumulation of algal-bacterial granular sludge. Bioresour. Technol. Rep. 7, 100228 https://doi.org/10.1016/j.biteb.2019.100228.
Meng, F., Xi, L., Liu, D., Huang, W., Lei, Z., Zhang, Z., Huang, W., 2019b. Effects of light intensity on oxygen distribution, lipid production and biological community of algal-bacterial granules in photo-sequencing batch reactors. Bioresour. Technol. 272, 473–481. https://doi.org/10.1016/j.biortech.2018.10.059.
Metz, B., Kossen, N.W.F., 1977. Growth of molds in from of pellets-literature-review. Biotechnol. Bioeng. 19 (6), 781–799. https://doi.org/10.1002/bit.260190602.
Muda, K., Aris, A., Salim, M.R., Ibrahim, Z., Yahya, A., van Loosdrecht, M.C., Ahmad, A., Nawahwi, M.Z., 2010. Development of granular sludge for textile wastewater treatment. Water Res. 44 (15), 4341–4350. https://doi.org/10.1016/j.watres.2010.05.023.
Nancharaiah, Y.V., Reddy, G.K.K., 2018. Aerobic granular sludge technology: Mechanisms of granulation and biotechnological applications. Bioresour. Technol. 247, 1128–1143. https://doi.org/10.1016/j.biortech.2017.09.131.
Peterson, G.L., 1977. Simplification of the protein assay method of Lowry et al-which is more generally applicable. Anal. Biochem. 83 (2), 346–356. https://doi.org/10.1016/0003-2697(77)90043-4.
Ramos, C., Suárez-Ojeda, M.E., Carrera, J., 2015. Long-term impact of salinity on the performance and microbial population of an aerobic granular reactor treating a high-strength aromatic wastewater. Bioresour. Technol. 198, 844–851. https://doi.org/10.1016/j.biortech.2015.09.084.
Ritchie, R.J., 2008. Universal chlorophyll equations for estimating chlorophylls a, b, c, and d. Photosynthetica 46 (1), 115–126.
Sengar, A., Aziz, A., Farooqi, I.H., Basheer, F., 2018. Development of denitrifying phosphate accumulating and anammox micro-organisms in anaerobic hybrid reactor for removal of nutrients from low strength domestic sewage. Bioresour. Technol. 267, 149–157. https://doi.org/10.1016/j.biortech.2018.07.023.
Sheng, G.P., Xu, J., Luo, H.W., Li, W.W., Li, W.H., Yu, H.Q., Xie, Z., Wei, S.Q., Hu, F.C., 2013. Thermodynamic analysis on the binding of heavy metals onto extracellular polymeric substances (EPS) of activated sludge. Water Res. 47 (2), 607–614. https://doi.org/10.1016/j.watres.2012.10.037.
Shi, Y., Liu, Y., 2021. Evolution of extracellular polymeric substances (EPS) in aerobic sludge granulation: composition, adherence and viscoelastic properties. Chemosphere 262, 128033. https://doi.org/10.1016/j.chemosphere.2020.128033.
Wang, H., Li, P., Jin, Q., Qin, G., 2014. Specific aerobic granules can be developed in a completely mixed tank reactor by bioaugmentation using micro-mycelial pellets of *Phanerochaete chrysosporium*. Appl. Microbiol. Biotechnol. 98 (6), 2687–2697. https://doi.org/10.1007/s00253-013-5261-7.
Wang, H., Li, P., Liu, G., Li, X., Yao, J., 2010. Rapid biodecolourization of eriochrome black T wastewater by bioaugmented aerobic granules cultivated through a specific method. Enzyme Microb. Technol. 47 (1-2), 37–43. https://doi.org/10.1016/j.enzmictec.2010.03.011.
Wang, L., Yu, T., Ma, F., Vitus, T., Bai, S., Yang, J., 2019. Novel self-immobilized biomass mixture based on mycelium pellets for wastewater treatment: a review. Water Environ. Res. 91 (2), 93–100. https://doi.org/10.1002/wer.1026.
Winkler, M.K., Kleerebezem, R., de Bruin, L.M., Verheijen, P.J., Abbas, B., Habermacher, J., van Loosdrecht, M.C., 2013. Microbial diversity differences within aerobic granular sludge and activated sludge flocs. Appl. Microbiol. Biotechnol. 97 (16), 7447–7458. https://doi.org/10.1007/s00253-012-4472-7.
Yu, T., Wang, L., Ma, F., Wang, Y., Bai, S., 2020. A bio-functions integration microcosm: self-immobilized biochar-pellets combined with two strains of bacteria to remove

atrazine in water and mechanisms. J. Hazard. Mater. 384, 121326 https://doi.org/10.1016/j.jhazmat.2019.121326.
Zhang, B., Guo, Y., Lens, P.N.L., Zhang, Z., Shi, W., Cui, F., Tay, J.H., 2019. Effect of light intensity on the characteristics of algal-bacterial granular sludge and the role of N-acyl-homoserine lactone in the granulation. Sci. Total Environ. 659, 372–383. https://doi.org/10.1016/j.scitotenv.2018.12.250.
Zhang, B., Lens, P.N.L., Shi, W., Zhang, R., Zhang, Z., Guo, Y., Bao, X., Cui, F., 2018. Enhancement of aerobic granulation and nutrient removal by an algal-bacterial consortium in a lab-scale photobioreactor. Chem. Eng. J. 334, 2373–2382. https://doi.org/10.1016/j.cej.2017.11.151.
Zhang, B., Li, W., Guo, Y., Zhang, Z., Shi, W., Cui, F., Lens, P.N.L., Tay, J.H., 2020a. A sustainable strategy for effective regulation of aerobic granulation: augmentation of the signaling molecule content by cultivating AHL-producing strains. Water Res. 169, 115193 https://doi.org/10.1016/j.watres.2019.115193.
Zhang, B., Li, W., Wu, L., Shi, W., Lens, P.N.L., 2022. Rapid start-up of photo-granule process in a photo-sequencing batch reactor under low aeration conditions: effect of inoculum AGS size. Sci. Total Environ., 153204 https://doi.org/10.1016/j.scitotenv.2022.153204.
Zhang, M., Ji, B., Liu, Y., 2021. Microalgal-bacterial granular sludge process: a game changer of future municipal wastewater treatment? Sci. Total Environ. 752, 141957 https://doi.org/10.1016/j.scitotenv.2020.141957.
Zhang, T., Shao, M.-F., Ye, L., 2012. 454 Pyrosequencing reveals bacterial diversity of activated sludge from 14 sewage treatment plants. Isme J. 6 (6), 1137–1147. https://doi.org/10.1038/ismej.2011.188.
Zhang, Y., Dong, X., Liu, S., Lei, Z., Shimizu, K., Zhang, Z., Adachi, Y., Lee, D.-J., 2020b. Rapid establishment and stable performance of a new algal-bacterial granule system from conventional bacterial aerobic granular sludge and preliminary analysis of mechanisms involved. J. Water Process Eng. 34, 101073 https://doi.org/10.1016/j.jwpe.2019.101073.
Zhao, Y., Guo, G., Sun, S., Hu, C., Liu, J., 2019a. Co-pelletization of microalgae and fungi for efficient nutrient purification and biogas upgrading. Bioresour. Technol. 289, 121656 https://doi.org/10.1016/j.biortech.2019.121656.
Zhao, Z., Liu, S., Yang, X., Lei, Z., Shimizu, K., Zhang, Z., Lee, D.J., Adachi, Y., 2019b. Stability and performance of algal-bacterial granular sludge in shaking photo-sequencing batch reactors with special focus on phosphorus accumulation. Bioresour. Technol. 280, 497–501. https://doi.org/10.1016/j.biortech.2019.02.071.
Zhao, Z., Yang, X., Cai, W., Lei, Z., Shimizu, K., Zhang, Z., Utsumi, M., Lee, D.J., 2018. Response of algal-bacterial granular system to low carbon wastewater: Focus on granular stability, nutrients removal and accumulation. Bioresour. Technol. 268, 221–229. https://doi.org/10.1016/j.biortech.2018.07.114.